JOURNAL OF MOLECULAR SPECTROSCOPY **188,** 14–26 (1998)
ARTICLE NO. MS977430

Far- and Mid-Infrared Emission Spectroscopy of LiH and LiD

M. Dulick,* K.-Q. Zhang,† B. Guo,† and P. F. Bernath†,[1]

**National Solar Observatory, National Optical Astronomy Observatories, P.O. Box 26732, Tucson, Arizona 85726; and †Centre for Molecular Beams and Laser Chemistry, Department of Chemistry, University of Waterloo, Waterloo, Ontario N2L 3G1, Canada*

Received May 16, 1997; in revised form August 14, 1997

High-resolution Fourier transform spectra of LiH and LiD were recorded in the far-infrared region, 100–360 cm^{-1}, and the mid-infrared regions, 800–1200 cm^{-1} and 2000–3000 cm^{-1}. A total of 261 pure rotational lines and 678 rovibrational lines were measured for the isotopomers ^{6}LiH(D) and ^{7}LiH(D). Molecular constants for the $X\,^1\Sigma^+$ ground state in the form of mass-dependent Dunham Y_{ij}'s and mass-independent Dunham U_{ij}'s were determined from a data set of 1476 lines, consisting of our measured line positions and previously reported microwave, millimeter-wave, and infrared lines. An effective internuclear potential for the ground electronic state where the Born–Oppenheimer part is modeled as a parameterized modified-Morse function was also determined from a fit of the data.

I. INTRODUCTION

Lithium hydride, the simplest of the metal-bearing diatomic molecules, has long attracted the interest of spectroscopists and theoreticians alike (*1, 2*). Ever since the inception of quantum chemistry, LiH has been the subject of numerous *ab initio* calculations, some of which served to validate various approximations used in calculating properties of electronic states of more complex diatomics (*3–11*). Because LiH is one of the lighter known heteronuclear diatomics, it is also becoming an important candidate in spectroscopic studies investigating the effects of breakdown in the Born–Oppenheimer approximation (*12–14*).

Lithium hydride may also be of prospective interest to astrophysicists as a means of monitoring the evolutionary cycle of the nucleosynthesis of light elements in stars or determining the primordial deuterium to hydrogen cosmic abundance ratio in interstellar clouds (*15*), an important concern to cosmologists in establishing whether the universe is open or closed. According to Wharton *et al.* (*16*), LiH has a large dipole moment of 5.882 D. As a result, submillimeter emission should be easy to detect in interstellar space. Furthermore, detecting submillimeter emission would not be hindered by the great quantities of dust and gas that frequently surround galactic cores, which are opaque to the transmission of visible light used to monitor the atomic absorption of lithium (the D lines). However, attempts to detect interstellar LiH(D) submillimeter emission so far have not been successful (*17*).

Prior to 1990, precise information about the properties of the $X\,^1\Sigma^+$ ground electronic state was obtained either directly from SCF calculations (*18–22*) or indirectly from the analysis of electronic spectra (*2, 23*) ($A\,^1\Sigma^+ - X\,^1\Sigma^+$ and $B\,^1\Pi - X\,^1\Sigma^+$). Only a handful of spectroscopic studies of limited scope were devoted exclusively to the $X\,^1\Sigma^+$ ground state. The combined microwave studies by Pearson and Gordy (*24*) and Plummer *et al.* (*25, 26*) managed to measure only the lowest $J = 0 \rightarrow 1$ and $J = 1 \rightarrow 2$ transitions for the first two vibrational states of the hydride and deuteride isotopomers. The low-resolution absorption infrared study by James *et al.* (*27*) established the ratio of the first two terms in the dipole moment expansion, while the diode laser spectra recorded by Yamada and Hirota (*28*) led to the refinement of the vibrational constants obtained from lower-resolution electronic spectra. Since then, Bellini and co-workers (*29, 30*) extended the number of hydride and deuteride rotational transitions measured in the millimeter region to higher J and v. In a similar fashion, Maki *et al.* (*31*) succeeded in measuring an extensive number of rotational absorption lines in both the far- and mid-infrared spectra with a Fourier transform spectrometer.

Maki *et al.* were unable to obtain a satisfactory fit of their infrared data to the Dunham potential. Subsequent treatments by Coxon (*13*) and Ogilvie (*14*) attributed the failure to inadequate treatment of J-dependent Born–Oppenheimer breakdown. For instance, using a variable-β Morse function to model the Born–Oppenheimer potential and power series expansions to correct for J-independent and J-dependent Born–Oppenheimer breakdown, Coxon was able to success-

[1] Also Department of Chemistry, University of Arizona, Tucson, AZ 85721.

0022-2852/98 $25.00

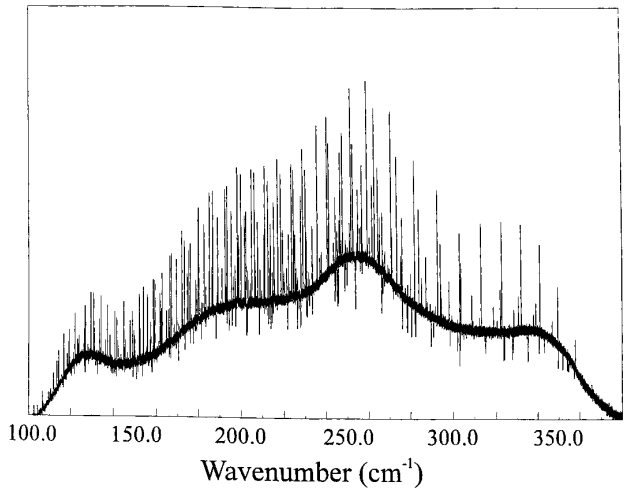

FIG. 1. An overview of the LiH(D) FTS spectrum in the far-infrared region.

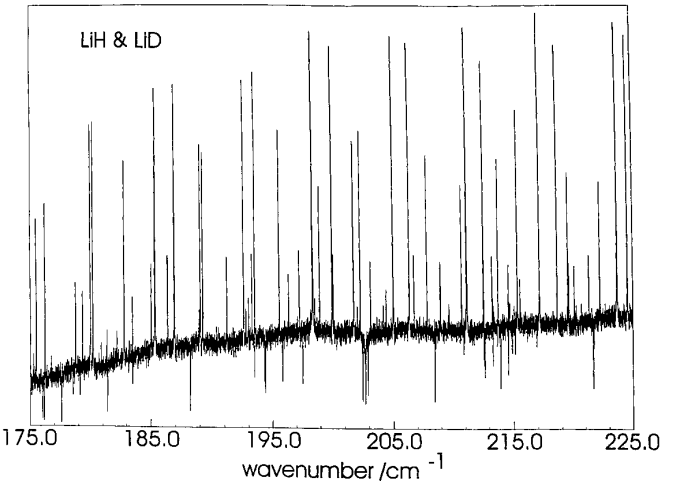

FIG. 2. An expanded portion of the LiH(D) FTS spectrum in the far-infrared region.

fully fit the data directly to the numerical eigenvalues of the radial Schrödinger equation to within experimental errors. Ogilvie followed a different approach, using analytical expressions instead to approximate the eigenvalues of the rovibrational levels (similar to the treatment used by Dunham) where both the Born–Oppenheimer potential and corrections

TABLE 1
^{6}LiH Infrared Transitions (cm^{-1})[a]

Line	Observed	δ	Line	Observed	δ	Line	Observed	δ	Line	Observed	δ	Line	Observed	δ
						(1,0) Band								
P(20)	1016.4017	5	P(19)	1035.8072	4	P(18)	1055.1624	2	P(17)	1074.4493	−13	P(16)	1093.6552	5
P(15)	1112.7571	4	P(14)	1131.7380	1	P(13)	1150.5794	0	P(12)	1169.2612	−3	P(11)	1187.7641	1
P(10)	1206.0670	4	P(9)	1224.1481	−1	P(8)	1241.9875	0	P(7)	1259.5632	1	P(6)	1276.8535	5
P(5)	1293.8356	1	P(4)	1310.4886	2	P(3)	1326.7896	−3	P(2)	1342.7200	23	P(1)	1358.2525	20
R(1)	1402.2633	6	R(2)	1416.0017	−3	R(3)	1429.2422	−1	R(4)	1441.9654	12	R(5)	1454.1497	5
R(6)	1465.7796	−2	R(7)	1476.8393	4	R(8)	1487.3100	−8	R(9)	1497.1797	−6	R(10)	1506.4344	8
R(11)	1515.0586	8	R(12)	1523.0422	12	R(13)	1530.3727	1						
						(2,1) Band								
P(20)	980.3118	2	P(19)	999.2130	9	P(18)	1018.0630	12	P(17)	1036.8444	2	P(16)	1055.5429	2
P(15)	1074.1398	−1	P(14)	1092.6175	−1	P(13)	1110.9575	3	P(12)	1129.1401	3	P(11)	1147.1451	−3
P(10)	1164.9541	−1	P(9)	1182.5457	1	P(8)	1199.8989	0	P(7)	1216.9940	13	P(6)	1233.8070	9
P(5)	1250.3175	3	P(4)	1266.5050	4	P(3)	1282.3482	14	P(2)	1297.8245	24	P(1)	1312.9098	6
R(0)	1341.8348	5	R(1)	1355.6380	69	R(2)	1368.9612	41	R(3)	1381.7915	−14	R(4)	1394.1196	−2
R(5)	1405.9201	6	R(6)	1417.1736	−10	R(7)	1427.8685	−3	R(8)	1437.9849	−13	R(9)	1447.5130	6
R(10)	1456.4352	18	R(11)	1464.7378	10	R(12)	1472.4199	90						
						(3,2) Band								
P(17)	999.9757	−9	P(16)	1018.1855	−2	P(15)	1036.2937	0	P(14)	1054.2833	3	P(13)	1072.1346	−8
P(12)	1089.8307	−16	P(11)	1107.3527	−19	P(10)	1124.6820	−5	P(9)	1141.7971	8	P(8)	1158.6758	4
P(7)	1175.3021	30	P(6)	1191.6485	19	R(3)	1335.3111	−10	R(4)	1347.2540	51	R(6)	1369.5471	−43
R(7)	1379.8869	31	R(8)	1389.6505	11	R(10)	1407.4222	−15						

[a] Observed − calculated differences (columns labelled δ) are in units of 0.0001 cm^{-1}.

TABLE 2
^{7}LiH Infrared Transitions (cm^{-1})[a]

Line	Observed	δ	Line	Observed	δ	Line	Observed	δ	Line	Observed	δ	Line	Observed	δ
						(1,0) Band								
P(28)	858.0924	−11	P(27)	877.0065	−24	P(26)	895.9782	−2	P(25)	914.9913	2	P(24)	934.0354	0
P(23)	953.0989	−1	P(22)	972.1691	2	P(21)	991.2319	2	P(20)	1010.2732	3	P(19)	1029.2782	3
P(18)	1048.2310	0	P(17)	1067.1161	1	P(16)	1085.9165	0	P(15)	1104.6148	−1	P(14)	1123.1935	−1
P(13)	1141.6337	−2	P(12)	1159.9171	0	P(11)	1178.0236	−3	P(10)	1195.9342	−2	P(9)	1213.6284	−2
P(8)	1231.0857	−2	P(7)	1248.2857	−1	P(6)	1265.2071	0	P(5)	1281.8291	0	P(4)	1298.1306	2
P(3)	1314.0902	3	P(2)	1329.6872	5	P(1)	1344.9005	6	R(0)	1374.0924	1	R(1)	1388.0321	6
R(2)	1401.5062	1	R(3)	1414.4975	1	R(4)	1426.9869	1	R(5)	1438.9564	−1	R(6)	1450.3894	−2
R(7)	1461.2695	−3	R(8)	1471.5815	−3	R(9)	1481.3108	−3	R(10)	1490.4437	−4	R(11)	1498.9683	−3
R(12)	1506.8724	−5	R(13)	1514.1464	−3	R(14)	1520.7805	−1	R(15)	1526.7661	−5	R(16)	1532.0969	−7
R(17)	1536.7673	−2	R(18)	1540.7717	1	R(19)	1544.1049	−10	R(20)	1546.7676	−4	R(21)	1548.7574	13
R(22)	1550.0721	24												
						(2,1) Band								
P(27)	844.9214	−16	P(26)	863.4188	0	P(25)	881.9559	16	P(24)	900.5190	10	P(23)	919.0974	−8
P(22)	937.6828	4	P(21)	956.2581	7	P(20)	974.8102	7	P(19)	993.3248	4	P(18)	1011.7910	42
P(17)	1030.1815	4	P(16)	1048.4916	3	P(15)	1066.7005	2	P(14)	1084.7909	2	P(13)	1102.7447	0
P(12)	1120.5438	1	P(11)	1138.1688	0	P(10)	1155.6009	1	P(9)	1172.8201	2	P(8)	1189.8063	1
P(7)	1206.5394	0	P(6)	1222.9990	2	P(5)	1239.1643	3	P(4)	1255.0146	4	P(3)	1270.5291	5
P(2)	1285.6872	6	P(1)	1300.4678	1	R(0)	1328.8187	5	R(1)	1342.3484	4	R(2)	1355.4215	−1
R(3)	1368.0208	4	R(4)	1380.1266	4	R(5)	1391.7219	1	R(6)	1402.7903	0	R(7)	1413.3159	0
R(8)	1423.2834	1	R(9)	1432.6784	−2	R(10)	1441.4885	1	R(11)	1449.7003	−1	R(12)	1457.3035	−1
R(13)	1464.2873	−2	R(14)	1470.6429	−1	R(15)	1476.3620	−3	R(16)	1481.4389	7	R(17)	1485.8639	−10
						(3,2) Band								
P(23)	885.7132	10	P(22)	903.8303	5	P(21)	921.9361	4	P(20)	940.0176	9	P(19)	958.0594	8
P(18)	976.0472	2	P(17)	993.9671	2	P(15)	1029.5367	0	P(14)	1047.1530	−3	P(13)	1064.6340	−8
P(12)	1081.9626	−3	P(11)	1099.1191	−3	P(10)	1116.0851	−2	P(9)	1132.8410	−3	P(8)	1149.3678	−1
P(7)	1165.6450	−2	P(6)	1181.6531	−1	P(5)	1197.3719	3	P(4)	1212.7805	3	P(3)	1227.8586	1
P(2)	1242.5865	3	P(1)	1256.9437	3	R(0)	1284.4686	21	R(1)	1297.5938	4	R(2)	1310.2715	−4
R(3)	1322.4835	−2	R(4)	1334.2108	−3	R(5)	1345.4358	−10	R(6)	1356.1442	−2	R(7)	1366.3176	−8
R(8)	1375.9434	−5	R(9)	1385.0062	−7	R(10)	1393.4944	−1	R(11)	1401.3946	0	R(12)	1408.6956	−5
R(13)	1415.3881	−9	R(14)	1421.4648	6	R(15)	1426.9154	16	R(16)	1431.7316	8	R(17)	1435.9093	−1
R(18)	1439.4452	5												
						(4,3) Band								
P(21)	888.1827	−2	P(20)	905.8117	2	P(19)	923.3994	4	P(18)	940.9307	−3	P(17)	958.3924	−6
P(16)	975.7707	9	P(15)	993.0454	0	P(14)	1010.2039	6	P(13)	1027.2269	3	P(12)	1044.0979	1
P(11)	1060.7993	6	P(10)	1077.3114	3	P(9)	1093.6163	2	P(8)	1109.6949	2	P(7)	1125.5271	−2
P(6)	1141.0945	3	P(5)	1156.3754	−3	P(4)	1171.3510	−9	P(3)	1186.0030	2	P(2)	1200.3083	−4
R(1)	1253.6882	−3	R(2)	1265.9767	−5	R(3)	1277.8076	9	R(4)	1289.1598	5	R(5)	1300.0196	12
R(6)	1310.3676	−2	R(7)	1320.1916	−6	R(8)	1329.4780	13	R(9)	1338.2089	10	R(10)	1346.3727	−3
R(11)	1353.9574	−23	R(12)	1360.9541	−35	R(14)	1373.1469	0						
						(5,4) Band								
P(15)	957.1371	−18	P(14)	973.8496	−40	P(13)	990.4345	10	P(12)	1006.8596	−22	P(11)	1023.1213	5
P(10)	1039.1925	−1	P(9)	1055.0603	14	P(8)	1070.7026	17	P(7)	1086.1011	15	P(6)	1101.2382	23
P(4)	1130.6442	11	P(3)	1144.8749	−1	R(4)	1244.8819	33	R(5)	1255.3722	−11	R(7)	1274.8456	46
R(8)	1283.7859	15												

[a] Observed − calculated differences (columns labelled δ) are in units of 0.0001 cm^{-1}.

TABLE 2—*Continued*

Line	Observed	δ	Line	Observed	δ	Line	Observed	δ	Line	Observed	δ	Line	Observed	δ
						(2,0) Band								
P(25)	2109.9377	2	P(24)	2138.2042	26	P(23)	2166.1591	1	P(22)	2193.7921	20	P(21)	2221.0754	7
P(20)	2247.9922	3	P(19)	2274.5202	−6	P(18)	2300.6397	0	P(17)	2326.3263	−4	P(16)	2351.5602	7
P(15)	2376.3154	1	P(14)	2400.5720	7	P(13)	2424.3048	5	P(12)	2447.4907	−1	P(11)	2470.1075	1
P(10)	2492.1298	−4	P(9)	2513.5362	3	P(8)	2534.3008	2	P(7)	2554.4007	0	P(6)	2573.8120	−8
P(5)	2592.5139	3	P(4)	2610.4797	−6	P(3)	2627.6887	−14	P(2)	2644.1212	1	P(1)	2659.7504	−11
R(1)	2701.6315	−2	R(2)	2713.8577	17	R(3)	2725.1816	−3	R(4)	2735.5938	14	R(5)	2745.0718	3
R(6)	2753.6048	5	R(7)	2761.1768	−5	R(8)	2767.7762	−15	R(9)	2773.3924	−22	R(10)	2778.0168	−11
R(11)	2781.6406	16	R(12)	2784.2492	−15	R(13)	2785.8439	−31						
						(3,1) Band								
P(22)	2116.8887	−11	P(21)	2143.5597	28	P(20)	2169.8624	28	P(19)	2195.7779	3	P(18)	2221.2904	4
P(17)	2246.3759	3	P(16)	2271.0130	2	P(15)	2295.1795	−1	P(14)	2318.8536	−1	P(13)	2342.0116	−9
P(12)	2364.6329	−4	P(11)	2386.6924	−6	P(10)	2408.1684	−3	P(9)	2429.0376	4	P(8)	2449.2748	−4
P(7)	2468.8607	8	P(6)	2487.7677	−5	P(5)	2505.9763	−10	P(4)	2523.4660	12	P(3)	2540.2090	6
P(2)	2556.1873	8	P(1)	2571.3789	11	R(0)	2599.3202	21	R(1)	2612.0271	−7	R(2)	2623.8738	17
R(3)	2634.8299	−38	R(4)	2644.8946	−10	R(5)	2654.0403	−22	R(6)	2662.2566	−28	R(7)	2669.5320	−11
R(8)	2675.8474	−39	R(9)	2681.1995	−33	R(10)	2685.5789	9	R(11)	2688.9689	6			
						(4,2) Band								
P(19)	2118.4492	2	P(18)	2143.3843	1	P(17)	2167.8961	−2	P(16)	2191.9644	1	P(15)	2215.5669	1
P(14)	2238.6813	−13	P(13)	2261.2902	7	P(12)	2283.3650	−6	P(11)	2304.8888	5	P(10)	2325.8354	1
P(9)	2346.1833	−7	P(8)	2365.9111	−8	P(7)	2384.9962	−1	P(6)	2403.4160	12	P(5)	2421.1431	−20
P(4)	2438.1650	−2	P(3)	2454.4538	4	R(1)	2524.1910	26	R(2)	2535.6579	9	R(3)	2546.2568	−4
R(4)	2555.9707	−19	R(5)	2564.7851	−27	R(6)	2572.6910	26	R(7)	2579.6578	−34	R(8)	2585.6921	−19
R(9)	2590.7759	0	R(10)	2594.8925	−47	R(11)	2598.0500	6						
						(5,3) Band								
P(16)	2114.2332	−23	P(15)	2137.3020	10	P(14)	2159.8820	−18	P(13)	2181.9613	−15	P(12)	2203.5182	16
P(11)	2224.5247	12	P(10)	2244.9634	18	P(9)	2264.8102	12	P(8)	2284.0471	35	P(7)	2302.6411	−25
P(6)	2320.5872	3	P(5)	2337.8537	20	P(4)	2354.4119	−47	P(2)	2385.3674	59	R(5)	2477.1366	18
R(6)	2484.7138	−30	R(7)	2491.3843	−7	R(8)	2497.1262	−10	R(9)	2501.9384	56	R(10)	2505.7907	−11
R(12)	2510.6315	−65	R(13)	2511.6122	3									
						(6,4) Band								
P(11)	2145.4022	−70	P(10)	2165.3501	−92	P(9)	2184.7219	−28	P(8)	2203.4809	−31	P(6)	2239.0929	−59
P(5)	2255.9117	0												

to the breakdown in the Born–Oppenheimer approximation are represented by series expansions involving the expansion variable $z = 2(R - R_e)/(R + R_e)$.

The purpose of this paper is to report new measurements of ^{6}LiH(D) and ^{7}LiH(D) infrared transitions from Fourier transform spectra in the far- and mid-infrared regions that were obtained by detecting emission rather than monitoring absorption. Most of the rotational transitions measured in the far-infrared spectra (278 lines) overlap with those measured by Maki *et al.* In the mid-infrared, $\Delta v = +1$ rovibrational transitions have now been extended up to vibrational levels $v = 5$ for ^{7}LiH and $v = 6$ for ^{7}LiD. In addition, we report the first overtone ($\Delta v = +2$) rotational lines of ^{7}LiH, which were measured successfully for the first time.

II. EXPERIMENT

The source for producing gas-phase lithium hydride consisted of an evacuated 1.2-m-long mullite tube with water-

TABLE 3
^{6}LiD Infrared Transitions (cm^{-1})[a]

Line	Observed	δ	Line	Observed	δ	Line	Observed	δ	Line	Observed	δ	Line	Observed	δ
						(1,0) Band								
P(25)	791.7279	10	P(24)	802.8759	2	P(23)	813.9958	−9	P(22)	825.0837	−5	P(21)	836.1299	−27
P(20)	847.1357	−1	P(19)	858.0896	20	P(18)	868.9826	7	P(17)	879.8114	−9	P(16)	890.5726	2
P(15)	901.2551	−3	P(14)	911.8544	−3	P(13)	922.3631	−3	P(12)	932.7751	6	P(11)	943.0804	−7
P(10)	953.2761	0	P(9)	963.3532	8	P(8)	973.3028	1	P(7)	983.1204	5	P(6)	992.7960	−7
P(5)	1002.3262	4	P(4)	1011.7011	10	P(3)	1020.9113	−9	R(3)	1080.2638	9	R(4)	1087.9234	−24
R(5)	1095.3642	−9	R(6)	1102.5760	14	R(7)	1109.5491	7	R(8)	1116.2790	−16	R(9)	1122.7652	−5
R(10)	1128.9963	−20	R(11)	1134.9735	1	R(12)	1140.6845	−16	R(13)	1146.1292	−25			
						(2,1) Band								
P(25)	770.6177	124	P(24)	781.5340	15	P(23)	792.4326	6	P(22)	803.2992	11	P(21)	814.1247	−5
P(20)	824.9084	10	P(19)	835.6388	−1	P(18)	846.3129	−5	P(17)	856.9249	2	P(16)	867.4657	−6
P(14)	888.3142	−5	P(13)	898.6084	2	P(12)	908.8039	−13	P(11)	918.8987	−6	P(10)	928.8828	−3
P(9)	938.7497	−1	P(8)	948.4928	4	P(7)	958.1036	1	P(6)	967.5741	−20	P(5)	976.9050	19
P(4)	986.0791	17	P(3)	995.0884	−33									
						(3,2) Band								
P(22)	781.8501	−5	P(21)	792.4610	−5	P(20)	803.0271	−9	P(19)	813.5446	8	P(18)	824.0033	1
P(17)	834.4002	3	P(16)	844.7274	−3	P(15)	854.9784	−18	P(14)	865.1503	−6	P(13)	875.2355	23
P(12)	885.2211	8	P(11)	895.1062	6	P(10)	904.8816	−5	P(9)	914.5454	24	P(8)	924.0831	19
P(7)	933.4898	1	P(6)	942.7598	−18									

[a] Observed − calculated differences (columns labelled δ) are in units of 0.0001 cm^{-1}.

cooled end windows made of either polyethylene for detecting far-infrared emission or KBr for detecting mid-infrared emission. The cell was heated by enclosing the central portion in a CM Rapid Temp tube furnace. Lithium hydride (or deuteride) was produced by reacting molten lithium, maintained at a temperature of 1050°C, with 20 Torr of hydrogen (or deuterium) gas. High-resolution spectra were recorded by detecting LiH(D) emission with a Bruker IFS 120 HR Fourier transform spectrometer that utilized a 3.5-μm Mylar beamsplitter and liquid helium-cooled bolometer detector in the far-infrared region, 100–360 cm^{-1}, and a KBr beamsplitter and a HgCdTe detector (800–1200 cm^{-1}) or an InSb detector (2000–3000 cm^{-1}) in the mid-infrared region. The resolution of the spectrometer was set to 0.01 cm^{-1}. Spectra were obtained by transforming interferograms constructed from 100 coadded scans for the far-infrared and 50 coadded scans for the mid-infrared. Two far-infrared spectra are displayed in Figs. 1 and 2.

Rotational line positions were measured using Brault's computer program PC-DECOMP and calibrated to absolute wavenumbers by impurity H_2O absorption lines present in all three spectra. Complete lists of measured ^{6}LiH(D) and ^{7}LiH(D) lines are given in Tables 1–5. The precision for the sharpest and most intense rotational lines listed in these tables (approximately 65%) is estimated to be 0.0005 cm^{-1}. In Table 5, pure rotational lines in the wavenumber range 100–130 cm^{-1} were measured to a precision no better than 0.005 cm^{-1}. A problem with the phase correction in transforming the one-sided interferogram in this wavenumber range reduced the precision of the measured line positions.

III. ANALYSIS

To determine the most precise empirical molecular constants for the $X\,^1\Sigma^+$ ground state required supplementing our set of infrared measurements with the Plummer *et al.* microwave lines, the Bellini *et al.* millimeter-wave lines, and the Maki *et al.* Fourier transform infrared lines, bringing the total number of lines in the dataset to 1476. Owing to the generally lower precision and redundancy with lines in the infrared Fourier transform spectra, the Yamada and Hirota and the Maki *et al.* lines from diode laser spectra were excluded. The Pearson and Gordy microwave lines were also

TABLE 4
^{7}LiD Infrared Transitions (cm^{-1})[a]

Line	Observed	δ	Line	Observed	δ	Line	Observed	δ	Line	Observed	δ	Line	Observed	δ
						(1,0) Band								
P(26)	771.9909	0	P(25)	782.7570	1	P(24)	793.4995	1	P(23)	804.2179	46	P(22)	814.8934	0
P(21)	825.5339	−1	P(20)	836.1299	2	P(19)	846.6747	0	P(18)	857.1631	−1	P(17)	867.5890	−1
P(16)	877.9462	−3	P(15)	888.2291	0	P(14)	898.4305	−1	P(13)	908.5446	−1	P(12)	918.5649	0
P(11)	928.4847	0	P(10)	938.2974	0	P(9)	947.9965	1	P(8)	957.5752	1	P(7)	967.0268	1
P(6)	976.3447	2	P(5)	985.5217	1	P(4)	994.5519	4	P(3)	1003.4277	4	P(2)	1012.1429	4
P(1)	1020.6903	0	R(0)	1037.2560	−17	R(1)	1045.2649	5	R(2)	1053.0779	−2	R(3)	1060.6928	4
R(4)	1068.1014	0	R(5)	1075.2994	1	R(6)	1082.2800	0	R(7)	1089.0383	0	R(8)	1095.5687	2
R(9)	1101.8628	−28	R(10)	1107.9245	−1	R(11)	1113.7402	−2	R(12)	1119.3091	2	R(13)	1124.6249	−4
R(14)	1129.6858	0	R(15)	1134.4862	−2	R(16)	1139.0241	5	R(17)	1143.2935	−5	R(18)	1147.2935	−9
R(19)	1151.0228	6	R(20)	1154.4757	12	R(21)	1157.6483	−10	R(22)	1160.5467	22	R(23)	1163.1581	−2
R(24)	1165.4899	8												
						(2,1) Band								
P(24)	772.8187	1	P(23)	783.3228	1	P(22)	793.7931	2	P(21)	804.2247	6	P(20)	814.6108	1
P(19)	824.9473	2	P(18)	835.2276	2	P(17)	845.4460	1	P(16)	855.5969	1	P(15)	865.6738	2
P(14)	875.6703	−1	P(13)	885.5811	3	P(12)	895.3987	0	P(11)	905.1174	1	P(10)	914.7304	2
P(9)	924.2312	2	P(8)	933.6133	2	P(7)	942.8701	4	P(6)	951.9946	3	P(5)	960.9807	4
P(4)	969.8213	5	P(3)	978.5098	3	P(2)	987.0393	−3	P(1)	995.4056	9	R(0)	1011.6154	16
R(1)	1019.4454	3	R(2)	1027.0865	6	R(3)	1034.5306	4	R(4)	1041.7725	5	R(5)	1048.8058	4
R(6)	1055.6248	2	R(7)	1062.2248	3	R(8)	1068.5998	4	R(9)	1074.7445	1	R(10)	1080.6545	1
R(11)	1086.3254	5	R(12)	1091.7509	−1	R(13)	1096.9291	3	R(14)	1101.8628	87	R(15)	1106.5222	−9
R(16)	1110.9331	8	R(17)	1115.0781	−2	R(18)	1118.9579	−2	R(19)	1122.5702	13	R(20)	1125.9096	13
R(21)	1128.9754	16												
						(3,2) Band								
P(21)	783.2431	9	P(20)	793.4235	−8	P(19)	803.5566	1	P(18)	813.6329	−3	P(17)	823.6482	−4
P(16)	833.5968	−1	P(15)	843.4721	0	P(14)	853.2679	−2	P(13)	862.9784	−3	P(12)	872.5982	4
P(11)	882.1190	1	P(10)	891.5356	0	P(9)	900.8423	7	P(8)	910.0305	2	P(7)	919.0961	9
P(6)	928.0301	3	P(5)	936.8270	−3	P(4)	945.4813	−2	P(3)	953.9859	1	P(2)	962.3329	−7
P(1)	970.5171	−14	R(0)	986.3746	6	R(1)	994.0316	−5	R(2)	1001.5013	−10	R(3)	1008.7784	−1
R(4)	1015.8547	−2	R(5)	1022.7259	4	R(6)	1029.3848	−3	R(7)	1035.8278	−2	R(8)	1042.0485	−5
R(9)	1048.0436	5	R(10)	1053.8056	2	R(11)	1059.3311	−1	R(12)	1064.6173	12	R(13)	1069.6554	−4
R(14)	1074.4476	12	R(15)	1078.9832	−10	R(16)	1083.2638	−17	R(17)	1087.2872	1	R(18)	1091.0457	−5
R(19)	1094.5406	8	R(20)	1097.7625	−30									
						(4,3) Band								
P(21)	762.5662	11	P(20)	772.5469	−5	P(19)	782.4809	8	P(18)	792.3571	−5	P(17)	802.1738	−5
P(16)	811.9240	−4	P(15)	821.6019	−1	P(14)	831.2010	−3	P(13)	840.7168	8	P(12)	850.1403	1
P(11)	859.4670	−3	P(10)	868.6914	0	P(9)	877.8055	−5	P(8)	886.8049	3	P(7)	895.6812	2
P(6)	904.4290	5	P(5)	913.0415	7	P(4)	921.5122	8	P(3)	929.8342	3	P(2)	938.0017	−3
P(1)	946.0092	1	R(1)	969.0074	47	R(2)	976.3035	−6	R(3)	983.4137	−3	R(4)	990.3264	−2
R(5)	997.0337	−26	R(6)	1003.5369	−5	R(7)	1009.8242	−5	R(8)	1015.8930	1	R(9)	1021.7373	2
R(10)	1027.3508	−16	R(11)	1032.7319	−23	R(12)	1037.8779	−4	R(13)	1042.7796	−7	R(14)	1047.4345	−19
R(15)	1051.8403	−26	R(16)	1055.9975	13									
						(5,4) Band								
P(18)	771.3772	15	P(17)	780.9989	8	P(16)	790.5546	2	P(15)	800.0382	−5	P(14)	809.4452	−1
P(13)	818.7679	−1	P(12)	828.0010	0	P(11)	837.1385	4	P(10)	846.1725	−5	P(9)	855.0998	2
P(8)	863.9126	11	P(7)	872.5983	−41	P(6)	881.1662	3	P(5)	889.5968	10	P(4)	897.8841	−15
P(3)	906.0289	−1	P(2)	914.0180	−18	R(2)	951.4644	−13	R(3)	958.4079	−32	R(4)	965.1638	24
R(5)	971.7106	−7	R(6)	978.0581	29	R(7)	984.1873	−5	R(8)	990.1032	−8			
						(6,5) Band								
P(15)	778.7567	16	P(14)	787.9743	12	P(13)	797.1092	12	P(12)	806.1541	4	P(11)	815.1059	16
P(10)	823.9535	−1	P(9)	832.6950	−5									

[a] Observed − calculated differences (columns labelled δ) are in units of 0.0001 cm^{-1}.

TABLE 5
Lithium Hydride and Deuteride $J \rightarrow J + 1$ Pure Rotational Transitions (cm^{-1})[a]

J	Observed	δ	J	Observed	δ	J	Observed	δ	J	Observed	δ	J	Observed	δ
						^{6}LiH								
						$v = 0$								
7	119.1642	26	8	133.5298	6	9	147.7149	−1	10	161.7012	0	11	175.4706	−2
12	189.0076	1	13	202.2956	1	14	215.3206	2	15	228.0682	1	16	240.5259	3
17	252.6812	4	18	264.5231	5	19	276.0412	6	20	287.2258	5	21	298.0684	0
22	308.5625	4	23	318.6995	−2	24	328.4764	11	25	337.8838	−1	26	346.9224	13
						$v = 1$								
7	115.6920	22	8	129.6339	5	9	143.4005	18	10	156.9680	−3	11	170.3264	10
12	183.4535	−6	13	196.3392	1	14	208.9664	3	15	221.3219	5	16	233.3930	6
17	245.1671	−1	18	256.6349	0	19	267.7859	4	20	278.6096	0	21	289.0996	5
22	299.2459	−6	23	309.0463	11									
						^{7}LiH								
						$v = 0$								
7	116.7833	78	8	130.8682	24	9	144.7807	−9	10	158.5049	−7	11	172.0205	−10
12	185.3120	−12	13	198.3652	−8	14	211.1649	−7	15	223.6949	−36	16	235.9572	51
17	247.9227	82	18	259.5753	2	19	270.9237	2	20	281.9515	7	21	292.6490	7
22	303.0096	9	23	313.0259	4	24	322.6930	5	25	332.0055	6	26	340.9587	5
27	349.5495	6	28	357.7753	10	29	365.6336	15						
						$v = 1$								
7	113.4128	43	8	127.0889	15	9	140.5959	8	10	153.9144	−3	11	167.0296	−4
12	179.9259	2	13	192.5871	0	14	205.0000	−1	15	217.1517	0	16	229.0293	−2
17	240.6224	3	18	251.9187	1	19	262.9101	7	20	273.5859	3	21	283.9391	2
22	293.9623	4	23	303.6483	1	24	312.9919	−2	25	321.9883	−3	26	330.6338	2
27	338.9227	−8	28	346.8557	1	29	354.4260	−17						
						$v = 2$								
7	110.1065	53	8	123.3767	7	9	136.4837	10	10	149.4055	6	11	162.1264	−3
12	174.6331	−1	13	186.9081	−15	14	198.9426	−1	15	210.7196	3	16	222.2278	2
17	233.4562	1	18	244.3950	4	19	255.0337	2	20	265.3639	1	21	275.3782	5
22	285.0681	1	23	294.4277	−7	24	303.4530	−2	25	312.1358	−19	26	320.4768	−8
27	328.4677	−20	28	336.1085	−26									
						$v = 3$								
9	132.4353	−37	10	144.9702	−1	11	157.3048	−2	12	169.4278	−5	13	181.3261	1
14	192.9852	3	15	204.3920	−2	16	215.5370	6	17	226.4065	3	18	236.9915	0
19	247.2831	2	20	257.2728	10	21	266.9504	0	22	276.3102	−15			

[a] Observed − calculated differences (columns labelled δ) are in units of 0.0001 cm^{-1}.

excluded, in this case, being superseded by the more accurate measurements of Plummer *et al.*

For the least-squares fits discussed below, our best lines, 65% of the 939 lines measured, were assigned a weighting factor of 0.0005 cm^{-1}. For the remainder of weaker and blended lines, the next two larger classes,

TABLE 5—*Continued*

J	Observed	δ	J	Observed	δ	J	Observed	δ	J	Observed	δ	J	Observed	δ
							^{6}LiD							
							$v = 0$							
12	110.3845	27	13	118.4512	15	14	126.4278	12	15	134.3082	12	16	142.0852	−2
17	149.7567	−2	18	157.3163	−2	19	164.7597	2	20	172.0816	2	21	179.2780	0
22	186.3449	−3	23	193.2795	3	24	200.0763	0	25	206.7331	−1	26	213.2485	17
27	219.6136	−5	28	225.8324	−1	29	231.8994	1	30	237.8131	7	31	243.5698	1
32	249.1705	11	33	254.6097	−1	34	259.8885	−9	35	265.0090	19	36	269.9602	−15
							$v = 1$							
13	115.8305	31	14	123.6250	10	15	131.3240	−14	16	138.9262	−3	17	146.4240	18
18	153.8068	−9	19	161.0773	−10	20	168.2281	−16	21	175.2568	−8	22	182.1575	−6
23	188.9285	10	25	202.0596	8	26	208.4152	9	28	220.6924	18	29	226.6062	−2
							^{7}LiD							
							$v = 0$							
13	114.3439	40	14	122.0601	37	15	129.6836	7	16	137.2151	7	17	144.6459	−2
18	151.9729	−4	19	159.1912	−3	20	166.2963	−3	21	173.2850	4	22	180.1513	−1
23	186.8910	−27	24	193.5077	0	25	199.9902	−3	26	206.3388	−1	27	212.5493	−8
28	218.6214	−1	29	224.5505	−1	30	230.3353	0	31	235.9740	5	32	241.4634	−1
33	246.8034	−1	34	251.9922	1	35	257.0281	1	36	261.9105	3	37	266.6377	0
38	271.2094	−4	39	275.6260	1	40	279.8853	0	41	283.9868	−12	42	287.9336	−2
43	291.7221	−3	44	295.3554	13									
							$v = 1$							
13	111.8602	53	14	119.4036	32	15	126.8585	14	16	134.2206	5	17	141.4848	0
18	148.6461	−4	19	155.7004	−5	20	162.6439	0	21	169.4713	−1	22	176.1796	−1
23	182.7652	0	24	189.2245	0	25	195.5549	4	26	201.7525	3	27	207.8147	0
28	213.7398	1	29	219.5245	0	30	225.1672	0	31	230.6658	1	32	236.0182	0
33	241.2230	−1	34	246.2792	3	35	251.1842	−3	36	255.9387	−2	37	260.5402	−6
38	264.9887	−11	39	269.2855	3	40	273.4272	7						
							$v = 2$							
13	109.4081	46	14	116.7810	8	15	124.0714	21	16	131.2671	9	17	138.3659	−2
18	145.3650	4	19	152.2576	3	20	159.0406	3	21	165.7091	−3	22	172.2610	−1
23	178.6919	0	24	184.9979	−4	25	191.1775	0	26	197.2264	3	27	203.1423	4
28	208.9222	2	29	214.5643	1	30	220.0663	−1	31	225.4273	6	32	230.6437	5
33	235.7143	0	35	245.4147	−5	36	250.0414	−13						
							$v = 3$							
13	106.9879	38	14	114.1965	23	15	121.3207	27	16	128.3518	11	17	135.2878	−1
18	142.1242	−10	19	148.8584	2	20	155.4830	0	21	161.9953	−4	22	168.3939	11
23	174.6693	−12	24	180.8265	5	25	186.8567	9	26	192.7565	−8	27	198.5287	10
28	204.1644	−1	29	209.6649	−6	30	215.0276	−10	31	220.2512	−7			

TABLE 6
Mass-Dependent Dunham Constants (cm^{-1})

	^{6}LiH	^{7}LiH	^{6}LiD	^{7}LiD
Y_{10}	1420.04763(55)	1405.49805(76)	1074.30876(76)	1054.93973(32)
Y_{20}	−23.595882(365)	−23.167899(714)	−13.516804(475)	−13.057768(208)
Y_{30}	0.1569973(684)	0.170928(281)	0.0705152(839)	0.0754777(497)
$10^3\ Y_{40}$		−1.7168(490)		−1.03907(392)
$10^4\ Y_{50}$		−1.1328(312)		
Y_{01}	7.67077959(171)	7.51373151(90)	4.39017060(206)	4.23308131(46)
Y_{11}	−0.22328990(462)	−0.21639109(243)	−0.09662406(489)	−0.091494283(839)
$10^3\ Y_{21}$	2.17707(302)	2.02305(192)	0.70332(245)	0.660793(426)
$10^5\ Y_{31}$	−4.6803(491)	−2.3166(574)	−1.0474(372)	−1.04033(550)
$10^6\ Y_{41}$		−2.2579(550)		
$10^4\ Y_{02}$	−8.949245(125)	−8.5858332(772)	−2.9312748(568)	−2.7259254(286)
$10^5\ Y_{12}$	1.69632(108)	1.592615(738)	0.418407(886)	0.383400(149)
$10^7\ Y_{22}$	−2.0688(340)	−1.0308(276)	−0.3326(224)	−0.34763(433)
$10^8\ Y_{32}$		−1.3581(307)		
$10^7\ Y_{03}$	1.151294(729)	1.079035(332)	0.2126204(899)	0.193654(123)
$10^9\ Y_{13}$	−1.1025(161)	−0.7635(117)	−0.15500(574)	−0.143210(685)
$10^{11}\ Y_{23}$		−5.963(223)		
$10^{11}\ Y_{04}$	−1.8937(156)	−1.69311(548)	−0.158995(433)	−0.17647(174)
$10^{13}\ Y_{14}$		−1.4020(677)		
$10^{15}\ Y_{05}$	2.793(103)	2.2296(296)		0.16182(958)
$10^{21}\ Y_{06}$				−9.11(182)

which constituted 21 and 11% of the total number of lines measured, were assigned weighting factors of 0.001 and 0.002 cm^{-1}, respectively. As for the Maki *et al.* data, the far-infrared lines, with the exception of 22 lines, were assigned a weighting factor of 0.0006 cm^{-1} and 82% of the mid-infrared lines a weighting factor of 0.0008 cm^{-1}. A weighting factor of 0.000003 cm^{-1} (90 kHz) was assigned for all but two of the microwave lines (three times the estimated uncertainty of 30 kHz quoted in Ref. (*25*)), with the exceptions being the ^{7}LiD $v = 0$ and ^{6}LiD $v = 1$ $J = 0 \rightarrow 1$ lines where weights of 0.000006 cm^{-1} (180 kHz) were used. Quoted uncertainties of the line positions from Ref. (*30*) for the most part served as weighting factors for the millimeter-wave lines. In the fits each datum was weighted with the square of the reciprocal of the estimated uncertainty.

The first set of molecular constants, the mass-dependent Dunham Y_{ij}'s listed in Table 6, were determined by fitting the lines of each individual isotopomer to (*32*)

$$E(v, J) = \sum_{i,j} Y_{ij}\left(v + \frac{1}{2}\right)^i [J(J+1)]^j. \qquad [1]$$

The normalized standard deviations were 1.0882 for the ^{6}LiD fit, 0.9762 for the ^{7}LiD fit, 0.8193 for the ^{6}LiH fit, and 0.7520 for the ^{7}LiH fit. The second set of molecular constants, the mass-independent Dunham U_{ij}'s given in Table 7, were determined from a global fit of the data to

$$E(v, J) = \sum_{i,j} \mu^{-(i+2j)/2} U_{ij}[1 + (m_e/M_A)\Delta_{ij}^A + (m_e/M_B)\Delta_{ij}^B]\left(v + \frac{1}{2}\right)^i [J(J+1)]^j, \qquad [2]$$

where Δ_{ij} are empirical Ross–Watson parameters that correct for Born–Oppenheimer breakdown on the lithium (A) and hydrogen (B) centers (*33–35*), μ is the reduced mass, M_A and M_B are the lithium and hydrogen atomic masses, and m_e is the electron mass. Unlike the Dunham Y_{ij} fits, the only adjustable parameters were the U_{i0}'s and U_{i1}'s while the remainder of U_{ij}'s were calculated from analytical relationships (*36*) that functionally depend on the U_{i0}'s and U_{i1}'s. The normalized standard deviation for this fit was 0.8697. Residuals of our measured line positions are given in Tables 1–5. To save space,

TABLE 7
Mass-Independent Dunham Constants (cm^{-1})

U_{10}	1319.94013(45)	$10^{12}\,U_{33}$	−3.85126181
U_{20}	−20.427978(318)	$10^{11}\,U_{04}$	−1.07328754
U_{30}	0.143602(126)	$10^{13}\,U_{14}$	−1.91050967
$10^{3}\,U_{40}$	−1.6875(216)	$10^{15}\,U_{24}$	1.58478889
$10^{5}\,U_{50}$	−6.264(135)	$10^{15}\,U_{34}$	1.68257707
U_{01}	6.62709992(97)	$10^{15}\,U_{05}$	1.81123821
U_{11}	−0.179107163(819)	$10^{17}\,U_{15}$	8.61693074
$10^{3}\,U_{21}$	1.583806(649)	$10^{18}\,U_{25}$	−2.61449968
$10^{5}\,U_{31}$	−2.0645(173)	$10^{19}\,U_{06}$	−3.43382105
$10^{6}\,U_{41}$	−1.1900(169)	$10^{20}\,U_{16}$	−3.00488869
$10^{4}\,U_{02}$	−6.68224015	$10^{21}\,U_{26}$	1.55676691
$10^{5}\,U_{12}$	1.16154705	$10^{23}\,U_{07}$	7.02992634
$10^{8}\,U_{22}$	−8.91354048	$10^{24}\,U_{17}$	8.83817944
$10^{9}\,U_{32}$	−4.07795202	$10^{26}\,U_{08}$	−1.52935877
$10^{10}\,U_{42}$	−2.70979204	$10^{27}\,U_{18}$	−2.37737547
$10^{8}\,U_{03}$	7.43077249	$10^{30}\,U_{09}$	3.46572223
$10^{10}\,U_{13}$	−4.46297373	$10^{34}\,U_{010}$	−8.07774327
$10^{11}\,U_{23}$	−2.29784448		
Δ^{Li}_{10}	−0.12407(265)	Δ^{H}_{10}	−0.723228(286)
		Δ^{H}_{20}	−0.51199(419)
Δ^{Li}_{01}	−0.12280(181)	Δ^{H}_{01}	−1.564991(154)
		Δ^{H}_{11}	−0.83724(550)
Δ^{Li}_{02}	−0.6741(343)	Δ^{H}_{02}	−3.9270(109)
		Δ^{H}_{12}	0.6964(792)
		Δ^{H}_{03}	−8.573(148)
		Δ^{H}_{04}	−10.510(610)

residuals corresponding to the microwave, millimeter-wave, and Maki *et al.* infrared lines are not listed here. Atomic masses from Ref. (*37*) were used for all of the computations.

In the final stage of the analysis an internuclear potential was determined from a fit of the observed data to the numerical eigenvalues of the radial Schrödinger equation,

$$\left\{\frac{\hbar^2}{2\mu}\frac{d^2}{dR^2} - U^{\text{eff}}(R) + E(v, J) - \frac{\hbar^2}{2\mu}[1 + q(R)]J(J+1)/R^2\right\}\psi(r; v, J) = 0,$$

using the form

$$U^{\text{eff}}(R) = U^{\text{BO}}(R) + U^{\text{C}}(R), \quad [3]$$

where

$$U^{\text{BO}} = D_e\{1 - \exp[-\beta(R)]\}^2/\{1 - \exp[-\beta(\infty)]\}^2 \quad [4]$$

is the Born–Oppenheimer potential modeled as a modified-Morse function (hereafter referred to as simply MMP),

$$\beta(R) = z\sum_{i=0}\beta_i z^i, \quad [5]$$

and

$$z = (R - R_e)/(R + R_e). \quad [6]$$

Born–Oppenheimer breakdown on the lithium and hydrogen centers is taken into account by the inclusion of J-independent terms,

$$U^{\text{C}}(R) = M_{\text{A}}^{-1}\sum_{i=1}u_i^{\text{A}}(R - R_e)^i + M_{\text{B}}^{-1}\sum_{i=1}u_i^{\text{B}}(R - R_e)^i, \quad [7]$$

and J-dependent terms,

$$q(R) = M_{\text{A}}^{-1}\sum_{i=0}q_i^{\text{A}}(R - R_e)^i + M_{\text{B}}^{-1}\sum_{i=0}q_i^{\text{B}}(R - R_e)^i. \quad [8]$$

The radial Schrödinger fit gave a normalized standard

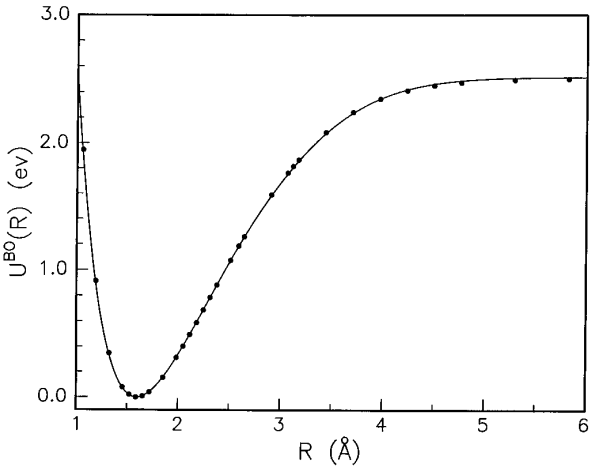

FIG. 3. Comparison of our experimentally determined MMP form of the Born–Oppenheimer potential with the Partridge and Langhoff ICSCF theoretical potential curve. The solid circles denote the theoretical values.

deviation of 0.8056. Determined potential parameters along with their uncertainties are displayed in Table 8, where the dissociation energy D_e was held fixed to the value used by Coxon (*13*) and the listed atomic masses were taken from Ref. (*37*). The Schrödinger equation was numerically integrated in the range $0.5 \leq R \leq 3.5$ Å, with a grid spacing of 0.001 Å.

Reliable information about the radial dependence of the Born–Oppenheimer potential of the $X\,^1\Sigma^+$ state has been amassed through numerous theoretical investigations. The comparison in Fig. 3 therefore is intended to show that MMP, a quantum-mechanical potential, is consistent with theoretical calculations. Of the more recent *ab initio* calculations reported on the $X\,^1\Sigma^+$ state of LiH, the Partridge and Langhoff ICSCF potential curve (*21*) is selected for this purpose because it is one of a few that were extensively tabulated over a wide range of internuclear separation and, moreover, served as a benchmark to gauge the results from more elaborate calculations. Because the ICSCF $^1\Sigma^+$ potential curve was reported in terms of total energy, to convert it to the energy scale of Fig. 3 required referencing it relative to its minimum at 3.0 au followed by scaling it so that the energy at 40 au coincided with $D_e = 20\,286.0$ cm^{-1} (2.5151 eV), which is slightly more (2%) than the calculated dissociation energy of 19 972 cm^{-1} reported in Ref. (*20*). It is clear from Fig. 3 that the shapes of the potential curves are in excellent agreement in the range of the observed spectrum, $1.2 \leq R \leq 2.5$ Å, and that this agreement is maintained well out to the dissociation limit.

Shown in Fig. 4 is the plot of the radial function $U^C(R)$ (Eq. [8]), the correction to breakdown in the Born–Oppenheimer approximation on both atomic centers. Because our model is based on Watson's treatment of an effective diatomic Hamiltonian for a Σ^+ state (35), $U^C(R)$ corrects for both adiabatic and nonadiabatic effects. We have also included in Fig. 4 for comparison the correction functions determined from a variety of different sources: the *ab initio* calculation by Bishop and Cheung (*38*), the analysis of optical A–X data by Chan *et al.* (*39*), the analysis of microwave and infrared data by Coxon (*13*), and the most recent analysis reported by Ogilvie (*14*), which in addition to microwave and infrared data also included the millimeter-wave lines of Bellini *et al.* (*30*). The experimentally determined curves agree with each other reasonably well in the range of our data. The most noticeable discrepancies occur past the outer end of the spectral range where our correction function in particular is no longer expected to provide reliable values. Since the theoretical curve furnishes information only on the adiabatic correction term, comparing it directly with the curves determined from experimental data indicates a substantial nonadiabatic contribution over much of the range of internuclear separation, as previously noted by Chan

TABLE 8
Derived Parameter Values for MMP

D_e (cm^{-1})	20286.0
R_e (Å)	1.594911495(145)
β_0	3.59992926(112)
β_1	3.2502445(294)
β_2	4.986672(188)
β_3	8.75569(170)
β_4	14.4769(135)
β_5	31.1700(583)
β_6	72.832(365)
u_1^{Li} (cm^{-1} u Å^{-1})	−2.5214(466)
u_2^{Li} (cm^{-1} u Å^{-2})	2.0261(752)
u_1^{H} (cm^{-1} u Å^{-1})	−35.20890(388)
u_2^{H} (cm^{-1} u Å^{-2})	43.4740(149)
u_3^{H} (cm^{-1} u Å^{-3})	−47.667(149)
u_4^{H} (cm^{-1} u Å^{-4})	57.500(404)
u_5^{H} (cm^{-1} u Å^{-5})	−59.388(583)
u_6^{H} (cm^{-1} u Å^{-6})	29.626(349)
q_1^{Li} (u Å^{-1})	0.0003447(154)
q_2^{Li} (u Å^{-2})	−0.0005119(471)
q_1^{H} (u Å^{-1})	0.00021722(271)
q_2^{H} (u Å^{-2})	0.00004583(750)
M (^{6}Li) (u)	6.0151214
M (^{7}Li) (u)	7.0160030
M (H) (u)	1.007825035
M (D) (u)	2.014101779

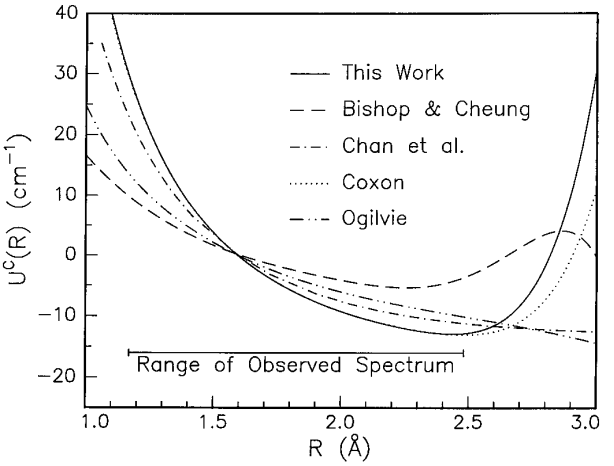

FIG. 4. A summary of reported adiabatic + nonadiabatic corrections to the Born–Oppenheimer potential for LiH. Note that the Bishop and Cheung theoretical curve only takes adiabatic corrections into account. The range of observed spectrum corresponds to our data set.

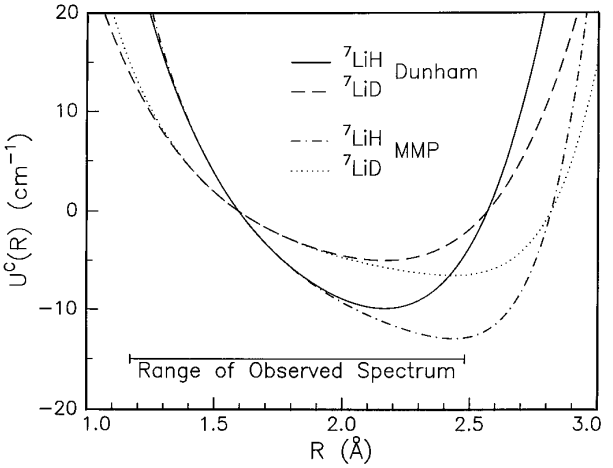

FIG. 5. The adiabatic + nonadiabatic corrections to the Born–Oppenheimer potential obtained from the semiclassical inversion of the Dunham energy levels. For comparison the corrections that correspond to the MMP form of the Born–Oppenheimer potential are also shown.

et al. (*39*). In the case of Ogilvie's curve the nonadiabatic contribution is only significant for $R > R_e$.

The empirical Ross–Watson delta parameters determined from the Dunham fit provide yet another means of independently confirming the results obtained from the radial Schrödinger fit. Using Watson's inversion formula (Eq. [49] in Ref. (*35*)) and the parameters in Table 7 gave the radial expansion parameters listed in Table 9. Plots of the correction function for ^{7}LiH and ^{7}LiD using the u's in Table 9 are shown in Fig. 5. In comparing these curves with those associated with MMP the agreement is excellent over 75% of the spectral range except at the outer end, starting at $R =$ 2 Å, where a much steeper rise is indicated by the correction functions associated with the delta parameters.

TABLE 9
Radial Expansion Parameters Derived from the Ross–Watson Delta Parameters

	Lithium Center	Hydrogen Center
u_1 (cm^{-1} u Å^{-1})	−2.598(499)	−35.200(707)
u_2 (cm^{-1} u Å^{-2})	2.477(973)	43.66(245)
u_3 (cm^{-1} u Å^{-3})		−41.40(805)
u_4 (cm^{-1} u Å^{-4})		34.6(102)
q_1 (u Å^{-1})	0.0002193(523)	0.000262179(112)
q_2 (u Å^{-2})		−0.00038442(250)
q_3 (u Å^{-3})		0.00038113(757)

ACKNOWLEDGMENTS

This work was supported in part by the Natural Sciences and Engineering Research Council of Canada (NSERC), the Petroleum Research Fund, administered by the American Chemical Society, and the NASA Laboratory Astrophysics Program.

REFERENCES

1. H. Hosoya, S. Yamabe, K. Morokuma, and K. Ohno, *J. Mol. Struct.* **289,** 1–100 (1993).
2. W. C. Stwalley and W. T. Zemke, *J. Phys. Chem. Ref. Data* **22,** 87–112 (1993).
3. A. M. Karo and A. R. Olson, *J. Chem. Phys.* **30,** 1232–1240 (1959).
4. F. E. Harris, *J. Chem. Phys.* **32,** 3–18 (1960).
5. W. H. Adams, *Phys. Rev.* **127,** 1650–1658 (1962).
6. J. C. Browne and F. A. Matsen, *Phys. Rev. A* **135,** 1227–1232 (1964).
7. W. A. Goddard, III, *Phys. Rev.* **157,** 73–80 (1967).
8. J. A. Keefer, J. K. Su Fu, and R. L. Belford, *J. Chem. Phys.* **50,** 160–173 (1969).
9. P. E. Cade and W. M. Huo, *J. Chem. Phys.* **47,** 614–648, 649–672 (1969).
10. C. F. Bender and E. R. Davidson, *Phys. Rev.* **183,** 23–30 (1969).
11. N. G. Mukherjee and R. McWeeny, *Int. J. Quantum Chem.* **4,** 97–107 (1970).
12. C. R. Vidal and W. C. Stwalley, *J. Chem. Phys.* **77,** 883–898 (1982).
13. J. A. Coxon, *J. Mol. Spectrosc.* **152,** 274–282 (1992).
14. J. F. Ogilvie, *J. Mol. Spectrosc.* **180,** 193–195 (1996).
15. N. Prantzos, E. Vangioni-Flam, and M. Cassé (Eds.), ''Origin and Evolution of the Elements,'' Cambridge Univ. Press, Cambridge, UK, 1993.
16. L. Wharton, L. P. Gold, and W. Klemperer, *J. Chem. Phys.* **52,** 2804 (1970).
17. P. de Bernardis, V. Dubrovich, P. Encrenaz, R. Maoli, S. Masi, G. Mastrantonio, B. Melchiorri, F. Melchiorri, M. Signore, and P. E. Tanzilli, *Astron. Astrophys.* **269,** 1–6 (1993).
18. K. K. Docken and J. Hinze, *J. Chem. Phys.* **57,** 4936–4952 (1972).
19. W. Meyer and P. Rosmus, *J. Chem. Phys.* **63,** 2356–2375 (1975).

20. B. Jönsson, B. O. Roos, P. R. Taylor, and P. E. M. Siegbahn, *J. Chem. Phys.* **74,** 4566–4575 (1981).
21. H. Partridge and S. R. Langhoff, *J. Chem. Phys.* **74,** 2361–2371 (1981).
22. B. O. Roos and A. J. Sadlej, *J. Chem. Phys.* **76,** 5444–5451 (1982).
23. K. P. Huber and G. Herzberg, ''Constants of Diatomic Molecules,'' Van Nostrand–Reinhold, New York, 1979.
24. E. F. Pearson and W. Gordy, *Phys. Rev.* **177,** 59–61 (1969).
25. G. M. Plummer, E. Herbst, and F. C. DeLucia, *J. Chem. Phys.* **81,** 4893–4897 (1984).
26. G. M. Plummer, E. Herbst, and F. C. DeLucia, *Astrophys. J.* **282,** L113–L114 (1984).
27. T. C. James, W. G. Norris, and W. Klemperer, *J. Chem. Phys.* **32,** 728–734 (1960).
28. C. Yamada and E. Hirota, *J. Chem. Phys.* **88,** 6702–6706 (1988).
29. M. Bellini, P. DeNatale, M. Inguscio, E. Fink, D. Galli, and F. Palla, *Astrophys. J.* **429,** 507 (1994).
30. M. Bellini, P. DeNatale, M. Inguscio, T. D. Varberg, and J. M. Brown, *Phys. Rev. A* **52,** 1954–1960 (1995).
31. A. G. Maki, W. B. Olson, and G. Thompson, *J. Mol. Spectrosc.* **144,** 257–268 (1990).
32. J. L. Dunham, *Phys. Rev.* **41,** 721–731 (1932).
33. A. H. M. Ross, R. S. Eng, and H. Kildal, *Opt. Commun.* **12,** 433 (1974).
34. J. K. G. Watson, *J. Mol. Spectrosc.* **45,** 99–113 (1973).
35. J. K. G. Watson, *J. Mol. Spectrosc.* **80,** 411–421 (1980).
36. J. Ogilvie, *Comput. Phys. Commun.* **30,** 101–105 (1983); private communication.
37. I. Mills, T. Cvităs, K. Homann, N. Kallay, and K. Kuchitsu, ''Quantities, Units, and Symbols in Physical Chemistry,'' Blackwell, Oxford, UK, 1988.
38. D. M. Bishop and L. M. Cheung, *J. Chem. Phys.* **79,** 2945–2950 (1983).
39. Y. C. Chan, D. R. Harding, and W. C. Stwalley, *J. Chem. Phys.* **85,** 2436–2444 (1986).